Reverse Electrowetting-on-Dielectric Energy Harvesting Using Inexpensive, Flexible Substrates

Baylee S. Schumacher, Pallav Kumar Sah, Karthik Kakaraparty, *Member, IEEE*, Ifana Mahbub, *Senior Member, IEEE*, and Russell C. Reid

***Abstract*—Reverse electrowetting-on-dielectric (REWOD) energy harvesting is an effective energy harvesting method at low frequencies such as the frequencies of human motion. Various REWOD energy harvester designs have been presented in prior works, but these generally use rigid and often expensive substrates and time-consuming and/or costly fabrication methods. To address these challenges, in this work REWOD energy harvesters were fabricated consisting of aluminized polyester sheets as the functional layers and with polycarbonate sheets for added mechanical support. The fabrication of these samples eliminates the need for costly materials, clean room technologies, and high-end equipment. Samples were characterized using a flat arrangement and on a test fixture that simulates the repeated bending that occurs on the back of a bending knee. Without applying any external bias voltage, the maximum voltage and current output for the bending samples were determined to be 25.1 mV and 230 nA, respectively, and the corresponding maximum power is 5.77 nW at a bending frequency of 5 Hz. With an estimated cost of U.S. $0.28 for each REWOD harvester (U.S. $0.03/cm^2), the cost per nanowatt of power is U.S. $0.05/nW, which is approximately 380 times lower than the approximately U.S. $19/nW of our previous REWOD energy harvesters. Our simple devices provide a low-cost, easily fabricated flexible approach to wearable motion sensing and energy harvesting that can be useful for various healthcare applications.**

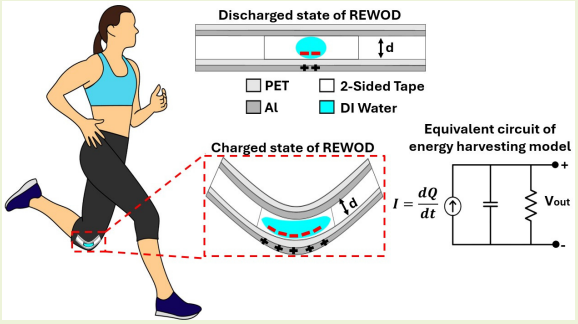

***Index Terms*— Energy harvesting, flexible substrates, motion sensor, reverse electrowetting-on-dielectric (REWOD).**

I. Introduction

IN THE rapidly evolving landscape of wearable technology, the quest for self-powered devices has become paramount. The rising costs associated with clean room assembly and the need to explore more cost-effective materials have spurred researchers to seek innovative solutions. At the heart of this endeavor lies the challenge of developing energy harvesting systems capable of generating reliable power while minimizing dependence on batteries, which often hinder device longevity and performance [1]. In this context, the emerging field of energy harvesting has witnessed significant advancements, with one particular technology garnering attention for its potential to revolutionize self-powered wearables: reverse electrowetting-on-dielectric (REWOD) [2], [3], [4], [5], [6], [7], [8], [9], [10], [11], [12], [13]. REWOD represents a promising avenue for energy harvesting in wearable devices, offering a unique combination of advantages that address critical limitations associated with traditional approaches. REWOD is related to electrowetting-on-dielectric (EWOD), but rather than producing liquid motion from an electrical input, REWOD produces an electrical output from liquid motion [1], [2], [3], [4], [14]. By harnessing the mechanical modulation of a liquid drop, REWOD brings forth the possibility of converting biomechanical motion/vibrations into electrical energy [5], [15], laying the foundation for self-sustaining wearable sensors.

The distinctive feature of REWOD lies in its ability to operate efficiently within low frequencies, typically encompassing a range directly relevant to the human body and its natural motion and activities, which are typically less than 10 Hz [16], [17]. This characteristic sets REWOD apart from many other energy-harvesting technologies that struggle to capture energy in this critical frequency band or rely on solid structures' resonance for optimal performance [18]. In preceding research, triboelectric nanogenerators (TENGs) have been called upon for these applications, which use the generation of electrical charges through the contact and

Manuscript received 22 July 2024; accepted 17 August 2024. Date of publication 5 September 2024; date of current version 16 October 2024. This work was supported by the National Science Foundation (NSF) under Grant ECCS 2246559. The associate editor coordinating the review of this article and approving it for publication was Prof. Tao Li. *(Corresponding author: Russell C. Reid.)*

Baylee S. Schumacher and Russell C. Reid are with the Department of Engineering, Utah Tech University, St. George, UT 84770 USA (e-mail: russell.reid@utahtech.edu).

Pallav Kumar Sah, Karthik Kakaraparty, and Ifana Mahbub are with the Department of Electrical and Computer Science Engineering, University of Texas at Dallas, Richardson, TX 75080 USA.

Digital Object Identifier 10.1109/JSEN.2024.3450430

separation of dissimilar materials [19], [20], [21]. This effect typically relies on contact between materials to create an electrostatic potential difference, leading to the flow of current and the conversion of mechanical energy into electrical energy. This results in significant material wear and fatigue and decreases the durability and reliability of the energy harvester [22]. Liquid–solid TENG mitigates some of the wear that occurs in solid–solid TENG [23], [24]. Liquid–solid TENG generally involves the repeated impacts of liquid on a solid dielectric surface and so the fundamental operating principle of TENG, which relies on friction or impact, remains unavoidable [18], [19]. Consequently, this characteristic poses a hindrance to the advancement of this technology.

REWOD offers the advantage of generating alternating current (ac) power without the need for an external bias source and without friction or impact between surfaces, leading to enhanced reliability and prolonged device lifespan. It must be mentioned that although an external bias source is not required for REWOD, an inherent bias of ∼10 mV does in fact exist between the REWOD liquid and the dielectric surface [25]. This inherent bias is responsible for increasing and decreasing the charge on the substrates as the liquid within the samples chamber is squeezed. The change in charge over time (dQ/dt) due to the mechanical modulation results in an electrical current, which is represented schematically in the graphical abstract.

The successful integration of REWOD technology into wearable sensors necessitates overcoming a series of challenges. In particular, the selection of suitable materials and electrode configurations, as well as the optimization of key parameters, such as dielectric properties, surface charge density, and electrode–electrolyte interfacial area. These parameters directly influence the capacitance in the dielectric material and the subsequent ac current generation in the REWOD system [1], [2], [3], [4]. To unlock the full potential of REWOD technology and pave the way for its practical implementation in self-powered wearables, interdisciplinary research efforts have flourished. The scientific community has made notable strides in exploring theoretical models, optimizing electrode–electrolyte configurations, and developing flexible electrodes [1], [5], [26]. This technology helps enable seamless integration of REWOD into wearable devices.

Considering these advancements, this research article aims to address one limitation of REWOD systems, which is their reliance on time-consuming and somewhat costly clean room technologies during device fabrication. This study uses inexpensive off-the-shelf materials that do not necessarily require a controlled processing and assembly environment, providing a cost-efficient alternative to conventional REWOD fabrication methods [1], [2], [3], [4]. Prior studies have primarily relied on the deposition of electrodes and dielectric coatings using physical vapor deposition on silicon substrates in a clean room environment or 3-D-printed formulated inks [1], [5], [26], [27]. In contrast, the present study aims to demonstrate that the reliance on clean room technology and expensive materials might be eliminated using inexpensive off-the-shelf components and facile fabrication and assembly. The utilization of disposable REWOD devices such as those in this research allows us to explore whether these devices can be scaled up depending on the application and amount of generated power required [8].

As electronics continue to shrink in size, the integration of efficient and flexible energy harvesting systems has become a pressing need [15], [28]. By leveraging the unique properties of REWOD technology, we strive to unlock a new paradigm in self-powered wearables—enabling devices that are not only flexible, reliable, and cost-efficient but also possess the ability to harvest energy from low-frequency human motion activities [1], [2], [3], [4], [15], [18]. In this article, a flexible system is at the forefront of the experiments and modeling to reexamine the theoretical aspects of REWOD, showcasing the development of an economical and flexible REWOD energy harvester. This system allows for an in-depth discussion of the advantages it offers and the challenges it poses. The novelty of this work is a flexible energy harvesting system that is easily accessible to a larger population due to facile, low-cost fabrication using commercially available materials and assembling without the use of a clean room or expensive equipment, while still producing a notable power density from low-frequency motion through bias-free REWOD. In addition, this article leverages a 3-D-printed, code-driven experimental test fixture, complemented by a simple yet accurate modeling process.

II. Materials and Methods

A. REWOD Experiments

All the experiments were performed using deionized (DI) water as the "electrolyte" and 50-μm-thick (0.002") aluminized polyester (PET) sheets (McMaster-Carr #7538T11) for the electrode and dielectric surfaces. The DI water was sandwiched between two aluminized polyester sheets with one side of the water touching the aluminized surface of one sheet and the opposite side of the water in contact with the PET surface of another sheet as shown in Fig. 1(a). For reference, a contact angle of approximately 72° is formed between the water and the PET surface [29]. For bending REWOD experiments, the aluminized films were separated by 3M 9474LE 300LSE double-sided tape, which also contained a void in it to define a chamber for the DI water. To make the bending REWOD samples more mechanically robust, the aluminized sheets were attached to 127 μm-thick polycarbonate (PC) sheets (McMaster-Carr #85585K73) using double-sided tape [see Fig. 1(b)]. Copper tape was used for electrical connections.

Two sets of experiments were performed to test the viability of the REWOD system in lower frequency motions. Flat REWOD experiments were performed to characterize the aluminized polyester sheet as an REWOD material. This established a baseline for comparison to previous similar REWOD experiments [1], [26], [27], [30]. Bending REWOD experiments were performed to simulate how the REWOD device would perform as a wearable energy harvester if, for example, it was adhered to the back of a person's leg behind their knee.

Flat REWOD experiments were performed using a custom mechanical oscillator consisting of a subwoofer speaker connected to an amplifier as shown in Fig. 2(b) and driven by a SIGLENT SDG 2042X function generator, similar to what

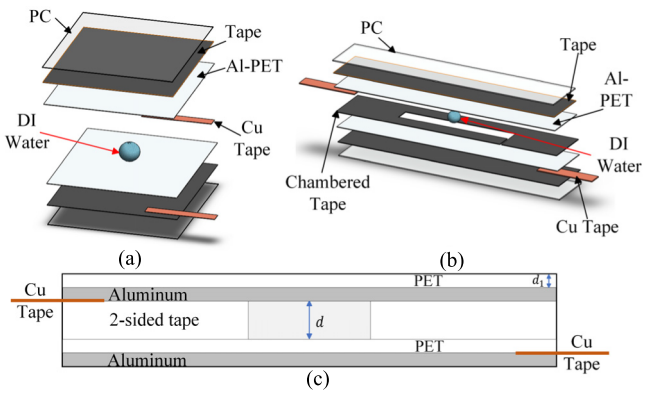

Fig. 1. Exploded view of samples. (a) Flat REWOD. (b) Bending REWOD. (c) Bending REWOD layers. d is the height of the REWOD chamber that contains the DI water and d_1 is the thickness of the PET dielectric layer.

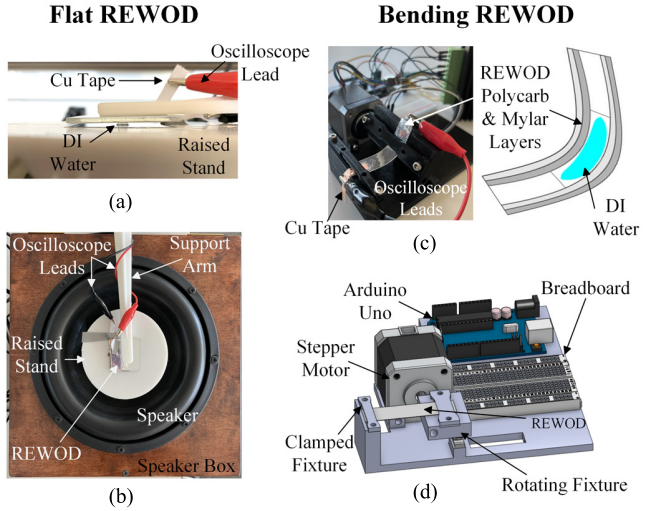

Fig. 2. Flat and bending REWOD test fixtures. (a) Side view of a flat REWOD sample with a DI water drop being squeezed. (b) Top view of the flat REWOD test fixture. (c) Isometric and section (photograph and schematic) views of the bending REWOD in the test fixture. (d) Isometric view of the bending REWOD test fixture.

was used for previous REWOD research [1], [26], [27], [31]. One aluminized polyester sheet was attached to the oscillator stage and another sheet was attached to a polycarbonate sheet (for rigidity) and then held above the oscillator. The aluminized polyester sheets were arranged in such a way that the aluminum surface of one sheet contacted the drop of DI water and the polyester surface of the other sheet contacted the drop, as illustrated in Fig. 2(a). Copper tape connected the aluminum surfaces to an oscilloscope (Keysight DSOX1204G). A 45-μL drop of DI water was placed between the sheets and the gap between sheets varied as the oscillator moved up and down, thus repeatedly squeezing the DI water drop without losing contact with the aluminized/polyester surfaces. The oscilloscope measured the voltage output during oscillation with various frequencies and oscillation amplitudes. A low-pass filter with a 20-Hz cutoff frequency was applied to the data because of the low signal-to-noise ratio.

Bending REWOD experiments were performed using a custom test fixture designed to hold a sample stationary on one end while the other end was bent, as illustrated in Fig. 2(d). An Arduino-controlled stepper motor was used to bend the samples to specific angles and at specified frequencies while the oscilloscope measured voltage output [see Fig. 2(c)]. Impedance magnitude and phase were measured with an Analog Devices AD5940 evaluation board, and the results were used to calculate output current, which is elaborated further in Section II-B.

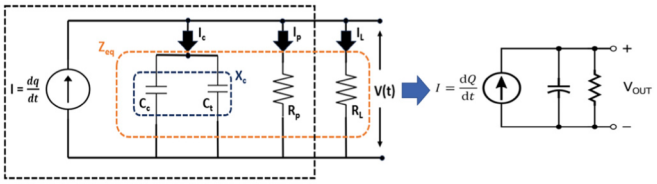

Fig. 3. REWOD equivalent circuit model.

B. Mathematical Modeling

Mathematical models were developed to describe how ac voltage is generated by squeezing DI water, which is what happens to the DI water in both the flat and bending REWOD experiments. In the flat REWOD case, the DI water is squeezed as the subwoofer speaker oscillates the raised stand holding one of the aluminized sheets up and down, while the other sheet is held stationary [see Fig. 2(a)]. In the bending REWOD case, the liquid is also squeezed but the squeezing occurs due to a mechanical bend of the samples from 0° to 90° and the differences in the radius of curvature of the top and bottom substrates. Illustrated in Fig. 1(c) is the arrangement of layers within the REWOD system, with d_1 representing the thickness of the PET and d representing the thickness of the chamber cut from the double-sided tape.

An electrical equivalent schematic of the REWOD energy harvester (REH) is shown in Fig. 3. The REWOD system generates an electric charge in response to mechanical modulation. As the modulation is applied to the system, the spacing d and the water-PET dielectric interfacial surface area A_s for a fixed volume of DI water change. Thus, the induced capacitance across the electrodes changes, correspondingly generating the alternating voltage and current. The mathematical relationship between the amount of charge generated and the change in capacitance is governed by (1) and (2):

$$q = CV \tag{1}$$

$$C = \frac{\epsilon_{\text{eff}}\epsilon_0}{d_1} A_s \tag{2}$$

where q is the generated charge, C is the variable capacitance, ϵ_0 is the free permittivity of a vacuum, and ϵ_{eff} is the effective combined relative permittivity of DI water and PET. ϵ_{eff} can be further defined by (3), with the values of the relative dielectric constants for DI water, ϵ_w, and PET, ϵ_p, given in Table I, which also contains descriptions and values of mathematical model parameters.

$$\epsilon_{\text{eff}} = \frac{d_1 + d_w}{\left(\frac{d_1}{\epsilon_p}\right) + \left(\frac{d_w}{\epsilon_w}\right)}. \tag{3}$$

In (3), d_w is the time-varying thickness of the water as the sample is being bent. The water thickness is the same as the distance between the top and the bottom of the REWOD

TABLE I
PARAMETERS USED FOR THE ANALYTICAL BENDING REWOD MODEL

Parameter	Description	Value
R_p	Parallel resistance	7.22 MΩ
R_L	Load resistance	11 kΩ
f	Oscillation frequency	1-5 Hz
ϵ_0	Free-space permittivity	8.85×10^{-12} F/m^2
ϵ_p	Relative permittivity of PET	3.25 [29]
ϵ_w	Relative permittivity water	78 [30]
d_1	PET film thickness	50 µm
Vol	DI water volume	6 µl
d_{min}	Minimum chamber height	2 µm
d_{max}	Maximum chamber height	170 µm

chamber in Fig. 1(c). Its value can be defined by the sinusoid function in (4) where the amplitude of the overall change in the thickness of the water is represented by d_m

$$d_w = d_m * \cos(\omega T) + (d_m + d_{\min}). \tag{4}$$

Conventional circuit diagrams typically do not incorporate "charge sources"; they primarily feature voltage sources and current sources. However, we have the capability to readily generate a current source by harnessing the charge produced by REH. Thus, to begin modeling of REH, it is important to remember that electric current, I, is the flow of electric charge in coulombs per second. Mathematically, it can be expressed as current being the derivative, or rate of change, of charge given in (5):

$$I = \frac{dq}{dt}. \tag{5}$$

As discussed before, the generated electric charge is due to the mechanical modulation of top and bottom electrodes, which form a capacitor. Since REH represents a dynamic combination of current source and variable capacitance, a more accurate presentation of the REH model would be to connect a parallel resistor across the source. This parallel resistor, R_p, corresponds to the leakage path for generated charge which gradually dissipates across the material.

The mechanical modulation of electrodes with a variable capacitor involves two components: a constant capacitance, maintained through consistent contact between the water and the top and bottom surfaces of the REWOD chamber, and a varying capacitance resulting from the oscillation of the top electrode and the varying electrode spacing, which alters the contact area with the electrolyte.

Hence, the variable capacitor can be modeled as a sinusoidal function based on its minimum and maximum capacitances for minimum and maximum separations in the chamber, $d_{\max}$ and $d_{\min}$, respectively. These are expressed in (6) and (7) where Vol is the fixed volume of the DI water and is expressed as $\text{Vol} = A_{\max} d_{\min} = A_{\min} d_{\max}$, where $A_{\min}$ and $A_{\max}$ represent the change in the water droplet surface area

$$C_{\max} = \frac{\epsilon_{\text{eff}} \epsilon_0}{d_{w,\min}^2} \text{Vol} \tag{6}$$

$$C_{\min} = \frac{\epsilon_{\text{eff}} \epsilon_0}{d_{w,\max}^2} \text{Vol}. \tag{7}$$

The variation in the system capacitance between $C_{\max}$ and $C_{\min}$ is represented as a sinusoidal function in (8) where C is the total capacitance of the system, C_c is the average of $C_{\max}$ and $C_{\min}$, and C_m is the amplitude of the variable capacitance due to oscillations. The angular frequency is $w = 2\pi f$ where f is the frequency of mechanical oscillations

$$C = C_c + C_m \sin(\omega t - \pi). \tag{8}$$

The above equation is divided into two parts: a constant capacitance, C_c, and the second term which is a sinusoidal function representing time-varying capacitance. Applying Ohm's law to Fig. 3, the generated sinusoidal voltage $V(t)$ can be expressed as

$$V(t) = I_c X_c = I_p R_p = I_L R_L \tag{9}$$

$$V(t) = (I_c + I_p + I_L) Z_{\text{eq}} \tag{10}$$

where I_P, I_L, R_P, and R_L are illustrated in Fig. 3, X_c is the net reactance of the system, Z_{eq} is the system equivalent impedance including the load derived from the configuration in Fig. 3 as

$$\frac{1}{Z_{\text{eq}}} = \frac{1}{X_c} + \frac{1}{R_p} + \frac{1}{R_L} \rightarrow Z_{\text{eq}} = \frac{X_c R_p R_L}{X_c R_p + R_p R_L + R_L X_c}. \tag{11}$$

From (9) and (10), it can be concluded that

$$V(t) = I_c \left(\frac{X_c}{R_L} + \frac{X_c}{R_p} + 1 \right) Z_{\text{eq}}$$
$$\left\{ I_L = \left(\frac{X_c}{R_L} \right) I_c \middle| I_p = \left(\frac{X_c}{R_p} \right) I_c \right\} \tag{12}$$

where the current, I_c, flowing through the variable capacitor can be expressed as

$$I_c = C \frac{dV(t)}{dt} + V(t) \frac{dC}{dt}. \tag{13}$$

The parallel capacitance C_p can be calculated using (14), and the parallel resistance R_p can then be obtained using the value of C_p in combination with (15). The remaining parameters being $|Z|$ the absolute impedance, and φ the phase angle

$$C_P = \frac{\tan(\varphi)}{\omega |Z| \sqrt{1 + \tan^2 \varphi}} \tag{14}$$

$$R_P = \frac{\tan(\varphi)}{-\omega C_P}. \tag{15}$$

For bending REWOD, $d_{\min}$ and $d_{\max}$ cannot be derived geometrically [25] because they are not only dependent on the curvature of the top and bottom substrates but also a result of material strain, particularly of the adhesive that holds the various layers together. A comprehensive SolidWorks finite element analysis (FEA) model of the bending REWOD samples used in this research was created to gain valuable insights with regard to the dynamic behavior of the DI water chamber as it undergoes bend angles ranging from 0° to 90°. This simulation provided knowledge regarding chamber height during bending, allowing for a deeper understanding of how the droplet's area changes, which is a key input for generating voltage as shown in the aforementioned equations. The model

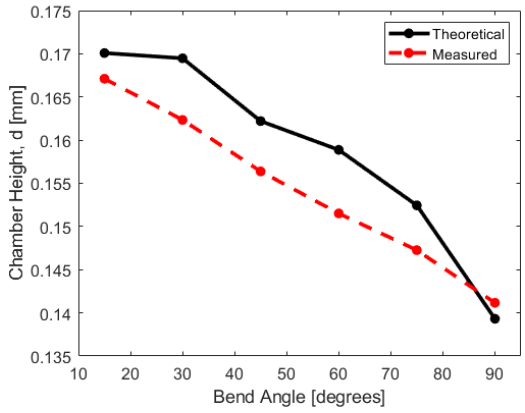

Fig. 4. SolidWorks chamber height through bend angles compared with measured chamber height of transparent samples.

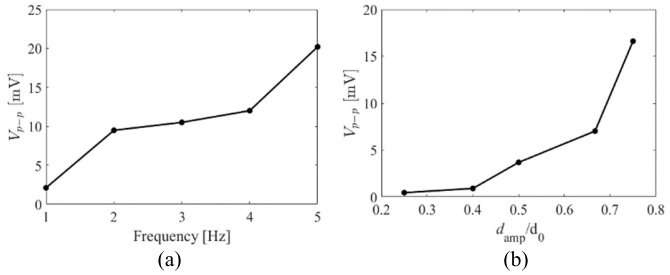

Fig. 5. Flat REWOD experimental peal-to-peak voltage data (a) versus frequency and (b) versus oscillation amplitude expressed as a ratio of the electrode oscillation amplitude and the initial distance between electrodes.

was also useful for predicting REWOD behavior for various sample lengths and widths.

Although the bending REWOD samples consist of various layers of differing materials, for simplicity the simulation assumed the REWOD sample was a single body. A fixed geometry constraint was placed at one end of the sample to mimic where it is securely held on a test stand and another fixed geometry constraint was located somewhat near the center of the DI water chamber to facilitate the bending shape observed on the test fixture. A displacement was applied to the edge of the sample opposite to the fixed edge to produce bending. Simulation probes were used to determine chamber height and the data were averaged for each of the seven bend angles: 0°–90°, with a step size of 15°. Transparent bending REWOD samples (without the aluminized polyester films) were used to validate the model results by placing a known volume of DI water inside a chamber and then estimating the liquid surface area to obtain d for each of the seven bend angles. Fig. 4 illustrates the results obtained through the FEA model compared with the results obtained from the transparent samples in terms of the change in chamber height. Based on these data, it is understood that the FEA predicts a similar change in chamber height compared with that calculated from the transparent samples.

III. Results

A. Flat REWOD

Flat REWOD voltage data show an increasing voltage with increasing oscillation frequency [see Fig. 5(a)] and with increasing oscillation amplitude [see Fig. 5(b)]. The voltage rises approximately 10× (from ∼2 to 20 mV) as the oscillation frequency increases from 1 to 5 Hz. The oscillation amplitude is plotted on the horizontal axis in Fig. 5(b) as a ratio versus the initial distance between electrodes, d_0. As the oscillation amplitude ratio increases from 0.25 to 0.75, the voltage increases approximately 30× (from ∼0.5 to 16.5 mV). In both the cases shown in Fig. 5, the increase in voltage is not linear due to liquid pinning on the electrode surfaces and also due to difficulties maintaining parallel top and bottom electrodes which affects the amount of liquid squeezing at different locations on the electrode during oscillations. The increase in voltage with frequency produces higher dC/dt and therefore higher current according to (13). Similarly, the increase in voltage with oscillation amplitude is the result of more dramatic liquid squeezing, which increases dC/dt and therefore current. The increase in voltage due to oscillation amplitude is more dramatic than due to oscillation frequency. This provides motivation for using flexible substrates in bending REWOD over rigid/flat REWOD because bending can dramatically modulate the distance between electrodes.

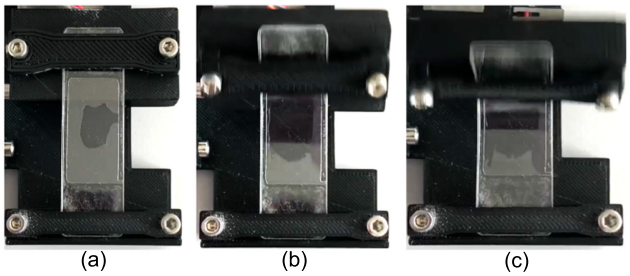

Fig. 6. Transparent samples. (a) No bend, (b) partial bend (∼45°), and (c) full bend (∼90°).

B. Bending REWOD

The SolidWorks FEA of bending REWOD indicated that wider REWOD chambers would result in increased droplet squeezing, leading to higher voltage output. However, initial voltage measurements did not support the FEA model's prediction. Rather than expanding across the surface area of the chamber, the DI water may have been drawn toward the sides or out of the chamber's air vent during the bending process. This occurrence may be the result of several factors, such as sagging in the center of the chamber with larger widths causing the water to move toward the edges even without bending, liquid pinning at the edges, and the influence of capillary action. To confirm this, transparent REWOD samples, without aluminized PET, were used for visual observation of DI water movement within the chamber as samples were bent. Some of the transparent samples are shown during bending in Fig. 6. This experimental approach confirmed that DI water often adheres to chamber sidewalls and this significantly decreases liquid deformation.

Using bending REWOD samples with chamber widths of 5, 10, 15, and 20 mm, voltage data were collected for each frequency ranging from 1 to 5 Hz. Fig. 7(a) illustrates the voltage results obtained for the various chamber widths across the stated frequency range. The samples with 10- and 15-mm-wide chambers produced the highest peak-to-peak voltages (V_{p-p}) with the 10-mm-wide chamber having the highest

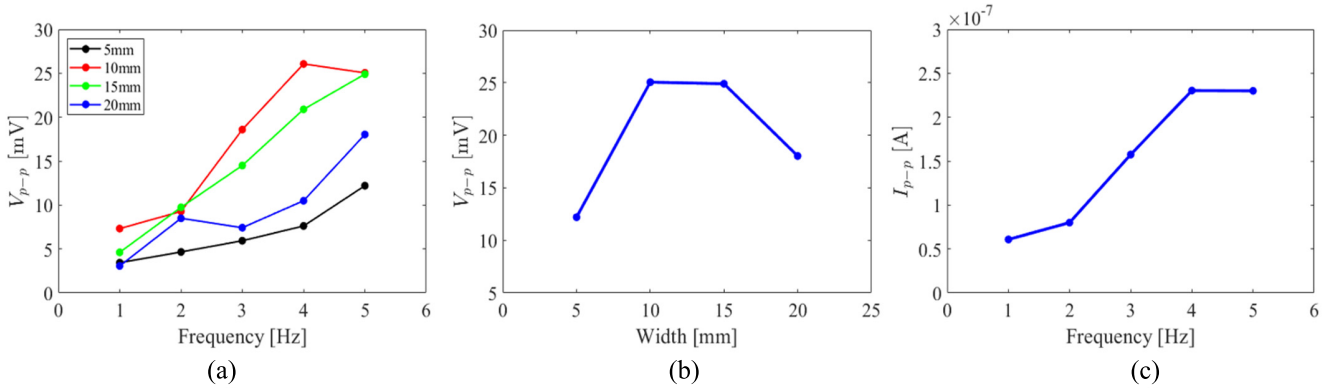

Fig. 7. Bending REWOD data. (a) Peak-to-peak voltage versus oscillation frequency for four chamber widths, (b) peak-to-peak voltage versus chamber widths at 5 Hz for 10-mm-wide samples, and (c) peak-to-peak current versus oscillation frequency for 10-mm-wide samples.

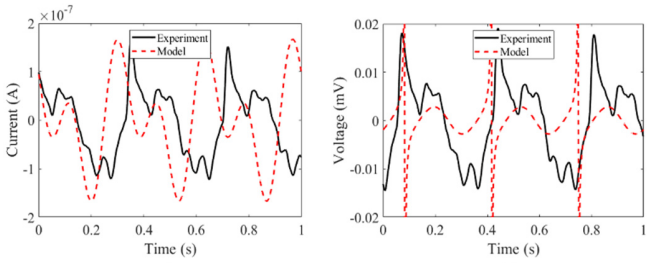

Fig. 8. MATLAB mathematical model versus experimental data. (a) Current versus time and (b) voltage versus time.

voltage of ~26 mV. Fig. 7(b) is a plot of V_{p-p} versus chamber width for an oscillation frequency of 5 Hz. These data, along with visual observations such as those shown in Fig. 6, demonstrate that in chambers wider than 10 mm, the liquid is not sufficiently squeezed, and therefore the voltage is lower. Based on these findings, additional samples with 10-mm-wide chambers were tested while collecting impedance data measured by the AD5940, which were then used along with the voltage measurements to calculate the current. The resulting data are shown in Fig. 7(c). Fig. 8 shows the current and voltage data plotted versus time alongside the analytical model's prediction.

Based on Fig. 7, a maximum V_{P-P} is obtained with an REWOD chamber width of 10 mm. At an oscillation frequency of 5 Hz, samples with this chamber width yielded a maximum V_{P-P} of 25.1 mV and a maximum current of 230 nA. The maximum power is therefore 5.77 nW, and the power density based on the chamber area (10 × 30 mm) is 1.92 nW/cm^2 Furthermore, the energy output was calculated to be 1.15 nJ/cycle.

IV. Discussion

Table II summarizes bias-free REWOD devices from the literature. Typical REWOD devices use a dielectric layer with a thickness in the tens of nanometers range [1]. The PET layer of our REWOD devices is 50 μm-thick—1000× thicker than what is typical for REWOD devices. As shown in (2), a thicker dielectric layer proportionally decreases the capacitance, and as a result, the current and power are lower, which is evident in Table II. The lower power output can be mitigated by leveraging the low-cost REWOD design and scaling up to produce sufficient power for specific applications.

TABLE II
Comparison of Recent Bias-Free REWOD

References	Dielectric and Thickness [μm]	Electrolyte	Oscillation Frequency [Hz]	Est. Power density [nW/cm^2]	Est. Cost [$/nW]*
Adhikari *et al.* [26]	Al_2O_3, 0.2	DI water	2	75	78
Kakarapar ty *et al.* [32]	Al_2O_3, 0.1	DI water	5	50	19
Adhikari *et al.* [27]	Al_2O_3, 0.15	DI water	5	3180	1
Moon *et al* [30]	PTFE, 0.3	DI water	10	300	--
This work	PET, 50	DI water	5	1.92	0.05

*For our previous works, $3,500 USD per 3 REWOD devices was used as an estimate for materials and clean room fees.

Another option is to evaluate additional commercial off-the-shelf metalized polymer films for REWOD or to experiment with using spin coating to deposit inexpensive dielectric layers for REWOD electrodes.

An often-neglected crucial aspect of novel energy harvesting technologies is their cost. The cost of energy harvesters is not often reported due to high material and processing costs but these are significant barriers to large-scale production and commercialization. The bending REWOD devices have overall dimensions of 6-cm-long and 1.35-cm-wide. Accounting for the cost of the various layers shown in Fig. 1, the bending REWOD devices cost U.S. $0.28 each, which is U.S. $0.03/cm^2. While energy harvesting cost is an important consideration, it should be put into the context of the power produced. The cost per power of the bending REWOD harvesters in material and processing costs is U.S. $0.05/nW. This is much lower than the cost-to-power ratio of our recent works—over 1500× less costly per nanowatt than [26] and 380× less costly than [32].

The low cost of these REWOD energy harvesters is one of their main advantages and opens the door to dramatic upscaling to suit the power requirements of various larger

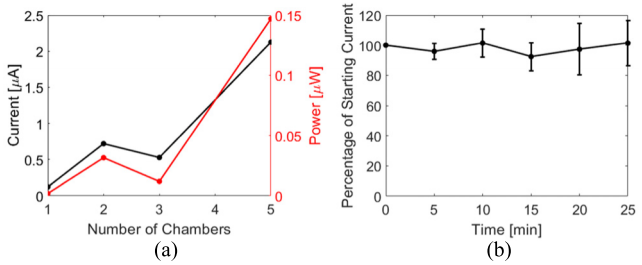

Fig. 9. (a) Bending REWOD current and power data at 3 Hz for the one-, two-, three-, and five-chamber samples. (b) Stability of generated current for a 25-min time period.

applications. Their ease of fabrication by not requiring clean room facilities or large/expensive equipment or processes is another advantage that makes these bendable REWOD harvesters highly scalable.

Design upscaling was explored by fabricating samples having two, three, or five chambers arranged side by side. The chamber dimensions matched the samples previously tested to determine the increase in harvested power as the system is scaled up. At a frequency of 3 Hz, the five-chamber samples had an average current of 2.13 μA and a power of 147 nW [see Fig. 9(a)], which is roughly a 20$\times$ increase from the one-chamber samples. The voltage remained constant as the samples were scaled up, as expected, because the chambers were arranged in parallel.

Upscaling is an important feature of these REWOD devices to compensate for their low power output, making them more practical. For example, wearable glucose sensors with power consumptions of 16 and 144 nW [33], [34] would require REWOD energy harvesters with areas 8.3 and 75 cm^2, respectively (as opposed to the 3-cm^2 device tested here). These are still small enough to be worn, especially if the REWOD energy harvesters are stacked rather than worn side by side.

Further testing was carried out regarding the stability of REWOD energy harvesting over 25 min to represent the system's performance during the length of time for a typical workout. These data are illustrated in Fig. 9(b). The data show that over the duration of time, the REWOD sample did not stray more than 8% from the original current.

V. Conclusion

This research has contributed to the development of flexible energy harvesting systems that have the possibility of being used for wearable technologies. This article has explored the limitations of previous REWOD systems, particularly those manufactured with more costly materials, equipment, and processes. In response to these limitations, this study presented an affordable approach using cost-efficient commercial off-the-shelf materials. With these readily available commercial materials, assembly does not require a controlled environment such as a clean room or expensive equipment, thus helping to make this technology more accessible and adaptable to a wider range of applications and researchers. The development of flexible electrode design and theoretical modeling has allowed for the improvement of this REWOD system. This work has revealed the significance of gap distance and chamber width in achieving higher power generation, marking a significant step forward in harnessing the full capabilities of this technology to power the next generation of wearable sensors. As electronics continue to shrink in size, the integration of efficient and flexible energy harvesting systems has become a pressing need. By achieving flexibility and cost-efficiency, this research contributes to facile self-powered wearables capable of harvesting energy from low-frequency human motion.

References

[1] P. R. Adhikari, N. T. Tasneem, R. C. Reid, and I. Mahbub, "Electrode and electrolyte configurations for low frequency motion energy harvesting based on reverse electrowetting," *Sci. Rep.*, vol. 11, no. 1, p. 5030, Mar. 2021, doi: 10.1038/s41598-021-84414-3.

[2] T.-H. Hsu, S. Manakasettharn, J. A. Taylor, and T. Krupenkin, "Bubbler: A novel ultra-high power density energy harvesting method based on reverse electrowetting," *Sci. Rep.*, vol. 5, no. 1, p. 16537, Nov. 2015, doi: 10.1038/srep16537.

[3] G. Kim, W. Kim, and H. Chun, "Droplet energy harvesting is reverse phenomenon of electrowetting on dielectric," *Adv. Funct. Mater.*, vol. 31, no. 43, Oct. 2021, Art. no. 2105233, doi: 10.1002/adfm.202105233.

[4] T. Krupenkin and J. A. Taylor, "Reverse electrowetting as a new approach to high-power energy harvesting," *Nature Commun.*, vol. 2, no. 1, p. 448, Aug. 2011, doi: 10.1038/ncomms1454.

[5] G. Carraro et al., "REWoD-based vibrational energy harvesting exploiting saline-solutions loaded PAAm hydrogels on micro-structured aluminium oxides electrodes," *Appl. Surf. Sci.*, vol. 611, Feb. 2023, Art. no. 155522, doi: 10.1016/j.apsusc.2022.155522.

[6] I. Sobianin, S. D. Psoma, and A. Tourlidakis, "A hybrid piezo-electric and electrostatic energy harvester for scavenging arterial pulsations," *Mater. Today, Proc.*, vol. 93, pp. 16–23, May 2023, doi: 10.1016/j.matpr.2023.05.213.

[7] H. Yang, H. Lee, Y. Lim, M. Christy, and Y.-B. Kim, "Laminated structure of Al_2O_3 and TiO_2 for enhancing performance of reverse electrowetting-on-dielectric energy harvesting," *Int. J. Precis. Eng. Manuf.-Green Technol.*, vol. 8, no. 1, pp. 103–111, Jan. 2021, doi: 10.1007/s40684-019-00145-x.

[8] I. Sobianin, S. D. Psoma, and A. Tourlidakis, "Recent advances in energy harvesting from the human body for biomedical applications," *Energies*, vol. 15, no. 21, p. 7959, Oct. 2022, doi: 10.3390/en15217959.

[9] A. Moyo, M. W. Shahzad, J. Terry, Y. Mita, and Y. Li, "A facile coplanar reverse electrowetting-on-dielectric configuration for more flexible and integratable force/motion sensing applications," in *Proc. IEEE Sensors*, Dallas, TX, USA, Oct. 2022, pp. 1–5, doi: 10.1109/SENSORS52175.2022.9967283.

[10] D. Singh, G. Bhutani, S. Sharma, and R. Kumar, "Energy harvesting through a low-cost device using reverse electrowetting on dielectric (REWOD)," in *Emerging Trends in Energy Conversion and Thermo-Fluid Systems* (Lecture notes in mechanical engineering), D. Sharma and S. Roy, Eds., Singapore: Springer, 2023, pp. 3–16, doi: 10.1007/978-981-19-3410-0_1.

[11] J. Jeong, B. Suh, and J. B. J. Lee, "A reverse electrowetting-on-dielectric (rewod) energy harvester using nonwetting gallium coated electrode and ultrathin gallium oxide shell as dielectric layer," in *Proc. IEEE 36th Int. Conf. Micro Electro Mech. Syst. (MEMS)*, Munich, Germany, Jan. 2023, pp. 693–696, doi: 10.1109/MEMS49605.2023.10052602.

[12] A. Moyo, M. W. Shahzad, J. G. Terry, S. Smith, Y. Mita, and Y. Li, "Test structures for studying coplanar reverse- electrowetting for vibration sensing and energy harvesting," in *Proc. 35th Int. Conf. Microelectron. Test Struct. (ICMTS)*, Tokyo, Japan, Mar. 2023, pp. 1–4, doi: 10.1109/ICMTS55420.2023.10094057.

[13] K. Kakaraparty, E. A. Pineda, B. Schumacher, R. C. Reid, and I. Mahbub, "Advanced bias-free energy harvesting based on high-dielectric flexible electrodes with reverse electrowetting-on-dielectric," *IEEE Sensors J.*, vol. 24, no. 7, pp. 9480–9488, Apr. 2024, doi: 10.1109/JSEN.2023.3345841.

[14] H. Cheng et al., "Robust reverse-electrowetting based energy harvesting on slippery surface," *RSC Adv.*, vol. 13, no. 45, pp. 31659–31666, 2023, doi: 10.1039/d3ra06099c.

[15] J. Yu, E. Ma, and T. Ma, "Harvesting energy from low-frequency excitations through alternate contacts between water and two dielectric materials," *Sci. Rep.*, vol. 7, no. 1, p. 17145, Dec. 2017, doi: 10.1038/s41598-017-17522-8.

[16] R. Khusainov, D. Azzi, I. Achumba, and S. Bersch, "Real-time human ambulation, activity, and physiological monitoring: Taxonomy of issues, techniques, applications, challenges and limitations," *Sensors*, vol. 13, no. 10, pp. 12852–12902, Sep. 2013, doi: 10.3390/s131012852.
[17] W. Ren, B. Peng, J. Shen, Y. Li, and Y. Yu, "Study on vibration characteristics and human riding comfort of a special equipment cab," *J. Sensors*, vol. 2018, pp. 1–8, Feb. 2018, doi: 10.1155/2018/7140610.
[18] R. Sun, S. Zhou, and L. Cheng, "Ultra-low frequency vibration energy harvesting: Mechanisms, enhancement techniques, and scaling laws," *Energy Convers. Manage.*, vol. 276, Jan. 2023, Art. no. 116585, doi: 10.1016/j.enconman.2022.116585.
[19] F. Xing, Y. Jie, X. Cao, T. Li, and N. Wang, "Natural triboelectric nanogenerator based on soles for harvesting low-frequency walking energy," *Nano Energy*, vol. 42, pp. 138–142, Dec. 2017, doi: 10.1016/j.nanoen.2017.10.029.
[20] J. Tan et al., "Advances in triboelectric nanogenerator powered electrowetting-on-dielectric devices: Mechanism, structures, and applications," *Mater. Today*, vol. 58, pp. 201–220, Sep. 2022, doi: 10.1016/j.mattod.2022.07.009.
[21] C. Wang et al., "Electrowetting-on-dielectric powered by triboelectric nanogenerator," *Nano Energy*, vol. 98, Jul. 2022, Art. no. 107310, doi: 10.1016/j.nanoen.2022.107310.
[22] J. Zhao and Y. Shi, "Boosting the durability of triboelectric nanogenerators: A critical review and prospect," *Adv. Funct. Mater.*, vol. 33, no. 14, Apr. 2023, Art. no. 2213407, doi: 10.1002/adfm.202213407.
[23] Z. Yuan and L. Guo, "Recent advances in solid–liquid triboelectric nanogenerator technologies, affecting factors, and applications," *Sci. Rep.*, vol. 14, no. 1, p. 10456, May 2024, doi: 10.1038/s41598-024-60823-y.
[24] Z. Lin, G. Cheng, L. Lin, S. Lee, and Z. L. Wang, "Water–solid surface contact electrification and its use for harvesting liquid-wave energy," *Angew. Chem. Int. Ed.*, vol. 52, no. 48, pp. 12545–12549, Nov. 2013, doi: 10.1002/anie.201307249.
[25] K. Kakaraparty, G. S. Hyer, E. A. Pineda, R. C. Reid, and I. Mahbub, "Theoretical modeling and experimental validation of reverse electrowetting on dielectric (REWOD) through flexible electrodes for self-powered sensor applications," in *Proc. IEEE Sensors*, Oct. 2022, pp. 1–4, doi: 10.1109/SENSORS52175.2022.9967270.
[26] P. R. Adhikari, M. N. Islam, Y. Jiang, R. C. Reid, and I. Mahbub, "Reverse electrowetting-on-dielectric energy harvesting using 3-D printed flexible electrodes for self-powered wearable sensors," *IEEE Sensors Lett.*, vol. 6, no. 5, pp. 1–4, May 2022, doi: 10.1109/LSENS.2022.3170207.
[27] P. R. Adhikari, A. B. Patwary, K. Kakaraparty, A. Gunti, R. C. Reid, and I. Mahbub, "Advancing reverse electrowetting-on-dielectric from planar to rough surface electrodes for high power density energy harvesting," *Energy Technol.*, vol. 10, no. 3, Mar. 2022, Art. no. 2100867, doi: 10.1002/ente.202100867.
[28] F. Zhu and O. G. Schmidt, "Editorial for a special issue 'Nano energy materials and devices for miniaturized electronics and smart system,'" *Nano Mater. Sci.*, vol. 3, no. 2, pp. 105–106, Jun. 2021, doi: 10.1016/j.nanoms.2021.06.004.
[29] *Critical Surface Tension and Contact Angle With Water for Various Polymers (Sort By Contact Angle)*. Accessed: Apr. 26, 2024. [Online]. Available: https://www.accudynetest.com/polytable_03.html?sortby=contact_angle
[30] J. K. Moon, J. Jeong, D. Lee, and H. K. Pak, "Electrical power generation by mechanically modulating electrical double layers," *Nature Commun.*, vol. 4, no. 1, p. 1487, Feb. 2013, doi: 10.1038/ncomms2485.
[31] N. T. Tasneem et al., "A self-powered wireless motion sensor based on a high-surface area reverse electrowetting-on-dielectric energy harvester," *Sci. Rep.*, vol. 12, no. 1, p. 3782, Mar. 2022, doi: 10.1038/s41598-022-07631-4.
[32] K. Kakaraparty, E. A. Pineda, R. C. Reid, and I. Mahbub, "Advancement of reverse electrowetting-on-dielectric with flexible electrodes for bias-free energy-harvesting applications," *IEEE Sensors J.*, vol. 23, no. 10, pp. 10334–10341, May 2023, doi: 10.1109/JSEN.2023.3264103.
[33] A. Tanaka, G. Chen, and K. Niitsu, "A 0.063-mm^2 1.75-nW biofuel cell-input biosensing/data-storing system with 5.5-GHz wireless backscatter data-readout in 65-nm CMOS for self-powered smart contact lenses," in *Proc. IEEE Biomed. Circuits Syst. Conf. (BioCAS)*, Oct. 2023, pp. 1–5, doi: 10.1109/BioCAS58349.2023.10388802.
[34] G. Chen, Y. Wang, T. M. Quan, N. Matsuyama, T. Tsujimura, and K. Niitsu, "A 0.5-mm^2 solar cell-powered biofuel cell-input biosensing system with LED driving for stand-alone RF-less continuous glucose monitoring contact lens," *IEEE Solid-State Circuits Lett.*, vol. 5, pp. 41–44, 2022, doi: 10.1109/LSSC.2022.3151904.
[35] V. I. Kuzkin, V. M. Elinson, O. I. Obrezkov, and Y. Y. Yakushkin, "Research of the dielectric properties of polyethyleneterephthalate modified by fluorocarbon films formed by ion-plasma technology methods," *J. Phys., Conf. Ser.*, vol. 1396, no. 1, Nov. 2019, Art. no. 012026, doi: 10.1088/1742-6596/1396/1/012026.
[36] G. A. Vidulich and R. L. Kay, "The dielectric constant of water between 0° and 40°," *J. Phys. Chem.*, vol. 66, no. 2, p. 383, Feb. 1962, doi: 10.1021/j100808a525.

Baylee S. Schumacher is currently pursuing the bachelor's degree in mechanical engineering with Utah Tech University, St. George, UT, USA. During her academic pursuits, she has developed a strong passion for material science, prototyping, manufacturing, and the complexities of high-level physics.

As she takes her first steps into the field of research, she is particularly captivated by the potential of REWOD energy harvesting on flexible electrodes and printable circuit technology.

Pallav Kumar Sah received the bachelor's degree in electrical engineering from the Maulana Abul Kalam Azad University of Technology, West Bengal, India, in July 2019, and the M.Sc. degree in electrical engineering from the Graduate Program, University of North Texas, Denton, TX, USA, in August 2022, where he is pursuing the Ph.D. degree with the Department of Electrical and Computer Engineering.

Before coming to Dallas, he worked on designing and developing an optimized control system for independent controls of inputs of the Doherty power amplifier. His research interests include RF circuits, wireless power transfer networks, wireless communication, and integrated circuit design.

Karthik Kakaraparty (Member, IEEE) is currently pursuing the Ph.D. degree with the Electrical and Computer Engineering Department, The University of Texas at Dallas, Richardson, TX, USA, under the supervision of Dr. Ifana Mahbub.

His current research interests include antenna technologies, REWOD energy harvesting based on flexible electrodes, and antenna designs for on-body flexible electronics-based applications.

Ifana Mahbub (Senior Member, IEEE) is an Assistant Professor and the Texas Instrument's Early Career Chair Awardee of the Department of Electrical and Computer Engineering, The University of Texas at Dallas, Richardson, TX, USA, where she is leading the Integrated Biomedical, RF Circuits and Systems Laboratory (iBioRFCASL). She has published two book chapters, 29 journal publications, and more than 62 peer-reviewed conference publications. Her research interests include energy-efficient integrated circuits and systems design for read-out, wireless communication, wireless power transfer for various implantable and wearable sensors, and ultrawideband/mm-wave phased-array antenna design for far-field wireless power transfer/V2V communication for UAVs.

Russell C. Reid received the bachelor's degree from Brigham Young University, Provo, UT, USA, in 2003, the master's degree from the University of Virginia, Charlottesville, VA, USA, in 2005, and the Ph.D. degree from The University of Utah, Salt Lake City, UT, USA, in 2016.

He is an Assistant Professor with the Department of Engineering, Utah Tech University, St. George, UT, USA. He has been or is currently the PI or Co-PI on federally funded grants and internally funded university grants. He has also been heavily involved in the development of the Engineering Department, Utah Tech University. His research interests include energy harvesting, biosensors, and electrowetting.